Crystal structures of ammonium citrates

Austin M. Wheatley,[1] and James A. Kaduk [1,2,a)]
[1]North Central College, 131 S. Loomis St., Naperville IL 60540, USA
[2]Illinois Institute of Technology, 3101 S. Dearborn St., Chicago IL 60616, USA

(Received 4 August 2018; accepted 24 October 2018)

The crystal structures of $(NH_4)H_2C_6H_5O_7$ and $(NH_4)_3C_6H_5O_7$ have been determined using a combination of powder and single crystal techniques. The structure of $(NH_4)_2HC_6H_5O_7$ has been determined previously by single crystal diffraction. All three structures were optimized using density functional techniques. The crystal structures are dominated by N-H···O hydrogen bonds, though O-H···O hydrogen bonds are also important. In $(NH_4)H_2C_6H_5O_7$ very strong centrosymmetric charge-assisted O-H-O hydrogen bonds link one end of the citrate into chains along the *b*-axis. A more-normal O-H···O hydrogen bond links the other end of the citrate to the central ionized carboxyl group. In $(NH_4)_2HC_6H_5O_7$, the very strong centrosymmetric O-H-O hydrogen bonds link the citrates into zig-zag chains along the *b*-axis. The citrates occupy layers parallel to the bc plane, and the ammonium ions link the layers through N-H···O hydrogen bonds. In $(NH_4)_3C_6H_5O_7$, the hydroxyl group forms a hydrogen bond to a terminal carboxylate, and there is an extensive array of N-H···O hydrogen bonds. The energies of the density functional theory-optimized structures lead to a correlation between the energy of an N-H···O hydrogen bond and the Mulliken overlap population: E(N-H···O) (kcal/mole) = 23.1(overlap)^{½}. Powder patterns of $(NH_4)H_2C_6H_5O_7$ and $(NH_4)_3C_6H_5O_7$ have been submitted to International Centre for Diffraction Data for inclusion in the powder diffraction file. © *2018 International Centre for Diffraction Data.* [doi:10.1017/S0885715618000829]

Key words: ammonium, citrate, powder diffraction, Rietveld refinement, density functional theory

I. INTRODUCTION

Our structural studies of Group 1 (alkali metal) citrates (Kaduk and Stern, 2016a, 2016b; Rammohan and Kaduk, 2016a, 2016b, 2016c, 2016d, 2016e, 2017a, 2017b, 2017c, 2017d, 2017e, 2017f; Rammohan *et al.*, 2016; 2017a, 2017b; Cigler and Kaduk, 2018) have led us to consider other citrate salts of monopositive cations. An ammonium ion is sometimes considered a pseudo-alkali metal cation.

To determine what crystallography had been done on ammonium citrates, we searched two databases. In the Powder Diffraction File (PDF)-4 Organics 2018 (Fawcett *et al.*, 2017), a search for compounds containing the elements H, C, N, and O only and "citrat" in the name yielded four hits. A search of the Cambridge Structural Database (Groom *et al.*, 2016) for entries containing both a citrate and an ammonium fragment yielded 23 hits, most of which also contained metal cations. For the purpose of this study, only four hits were relevant.

The unit cell of $(NH_4)H_2C_6H_5O_7$ was reported by Love and Patterson (1960; CSD Refcode ZZZDTW): space group *P-1*, $a = 7.492$, $b = 10.539$, $c = 6.150$ Å, $\alpha = 102.42$, $\beta = 105.57$, $\gamma = 104.67°$, $V = 431.145$ Å^3, $Z = 2$, but no atom coordinates were determined.

The crystal structure of $(NH_4)_2HC_6H_5O_7$ was reported by Andrade *et al.* (2002; CSD Refcode ZZZSAC01). The space group is *Pnma*, with $a = 10.775(6)$, $b = 14.715(7)$, $c = 6.165(2)$ Å, $V = 977.5$ Å^3, and $Z = 4$. The unit cell had been reported previously by Love and Patterson (1960). Experimental powder patterns of diammonium hydrogen citrate were reported by Visser (1979) and Gong (1980), and a pattern calculated from the crystal structure is included in the PDF-4 Organics as entry 02-081-0712.

An orthorhombic unit cell with $a = 6.2232$, $b = 15.048$, and $c = 11.056$ Å was reported for $(NH_4)_3C_6H_5O_7$ by Venkateshwarlu *et al.* (1989; CSD Refcode SESJIJ), but no coordinates were determined. An experimental powder pattern is reported by Venkateshwarlu *et al.* (1993) as PDF entry 00-045-1540 with a space group *Pcc2*, $a = 6.171(2)$, $b = 14.990(6)$, $c = 10.783(5)$ Å, $V = 997.46$ Å^3. Both the unit cell and the powder pattern make it clear that this material is actually $(NH_4)_2HC_6H_5O_7$ (Figure 1).

II. EXPERIMENTAL

$(NH_4)H_2C_6H_5O_7$. To 2.0281 g citric acid monohydrate (10.0 mmoles, Sigma-Aldrich lot #089K0091) dissolved in 10 ml water were added 2.3735 g (30.0 mmoles, Spectrum Chemical lot#00B34) NH_4HCO_3. After fizzing, the clear solution was exposed to ambient conditions in a Petri dish in a fume hood. After 18 days, a white solid was observed in the thick solution (20307-106-1). Single crystals (20307-105-1) were obtained from a replication of this preparation. The composition of the crystals did not correspond to the overall stoichiometry.

A portion of the solid was ground in a mortar and pestle. The X-ray powder pattern was measured on a Bruker D2 Phase diffractometer equipped with a LynxEye position-sensitive detector. The pattern was measured using Cu*Kα*

a)Author to whom correspondence should be addressed. Electronic mail: kaduk@polycrystallography.com

https://doi.org/10.1017/S0885715618000829 Published online by Cambridge University Press

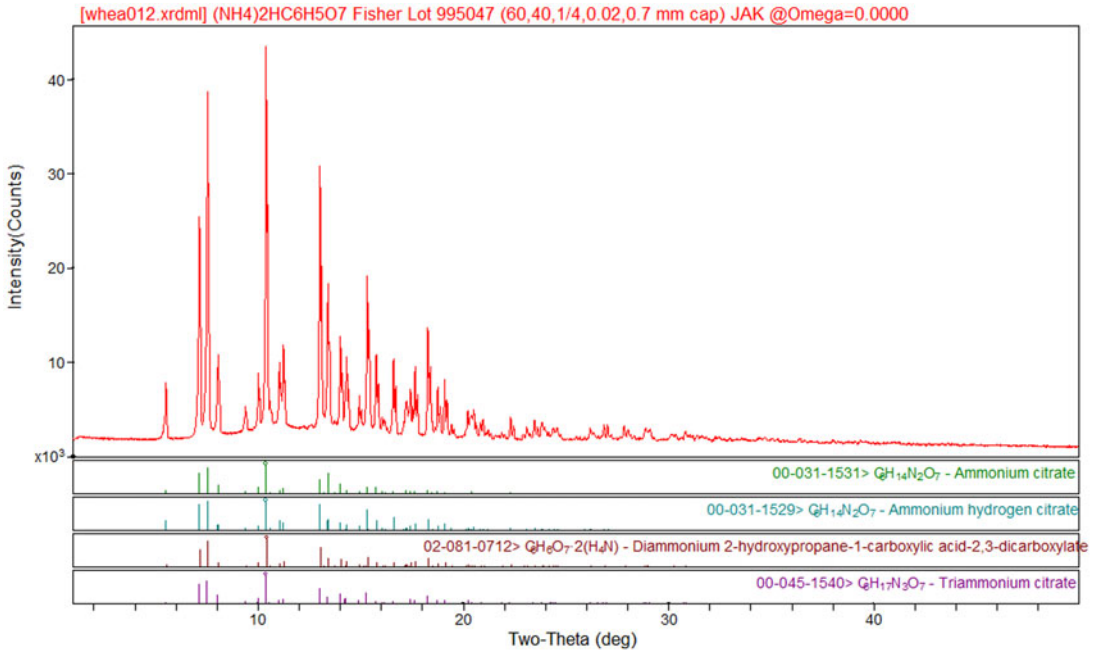

Figure 1. (Color online) Experimental powder pattern of $(NH_4)_2HC_6H_5O_7$ (Mo K_α radiation), with the three PDF entries for this compound. The "triammonium citrate" of PDF entry 00-045-1540 has been mis-characterized.

radiation from 5 to 100°2θ in 0.0202144° steps, counting for 0.5 s/step. The standard instrument settings (30 kV, 10 mA, 0.6 mm divergence slit, 2.5°Soller slits, and 3 mm scatter screen height) were employed.

The powder pattern was indexed on a primitive triclinic unit cell with $a = 6.1166$, $b = 7.4765$, $c = 10.5035$ Å, $\alpha = 104.791$, $\beta = 101.744$, $\gamma = 105.730°$, $V = 427.4$ Å^3 using N-TREOR as incorporated into EXPO2014 (Altomare *et al.*, 2013). This cell is very similar to the reduced cell reported by Love and Patterson (1960) for $(NH_4)H_2C_6H_5O_7$ ($a = 6.150$, $b = 7.492$, $c = 10.539$ Å, $\alpha = 104.67$, $\beta = 102.42$, $\gamma = 105.57°$, $V = 431.145$ Å^3), indicating that ammonium dihydrogen citrate crystallized from an aqueous solution of triammonium citrate. The structure was solved with FOX (Favre-Nicolin and Černý, 2002) using an ammonium cation and a citrate anion as fragments. The positions of the active hydrogens were deduced by analysis of hydrogen bonding patterns.

Subsequent to the solution using powder data, single crystals were obtained from another crystallization from triammonium citrate solution. A crystal approximately $0.20 \times 0.30 \times 0.50$ mm^3 was mounted in a Bruker SMART X2S diffractometer, and a single crystal data set was collected at 300 K using MoK_α radiation. Data collection information is summarized in Table I.

Since the single crystal and powder data sets were collected at the same temperature, a joint refinement using both data sets was carried out using GSAS (Toby, 2001; Larson and Von Dreele, 2004). Only the 12.0–100.0° portion of the powder pattern was included in the refinement ($d_{min} = 1.005$ Å). The C, N, and O atoms were refined independently and anisotropically. The C-H bond distances were restrained to 0.96(2) Å, the O17-H18 distance to 0.85(2) Å, and the N-H distances to 0.95(2) Å. The hydrogen atoms were refined isotropically, with common U_{iso} based on chemical similarity. The peak profiles were described using profile function #4 (Thompson *et al.*, 1987; Finger *et al.*, 1994), which includes the Stephens (1999) anisotropic strain broadening model. The background was modeled using a 6-term shifted Chebyshev polynomial. A 4th-order spherical harmonic model was included; the refined texture index was 1.114, so preferred orientation was present in the powder specimen. The final refinement of 177 variables using 8119 observations (4353 powder data points, 3757 single crystal reflections, and

TABLE I. Single crystal data collection for $(NH_4)H_2C_6H_5O_7$.

Identification code	20307-105-1	
Empirical formula	$C_6H_{11}N_2O_7$	
Formula weight	212.08	
Temperature	300(2) K	
Wavelength	0.71073 Å	
Crystal system	Triclinic	
Space group	*P-1*	
Unit cell dimensions	$a = 6.1203(10)$ Å	$\alpha = 104.865(6)°$
	$b = 7.4544(14)$ Å	$\beta = 101.744(5)°$
	$c = 10.469(2)$ Å	$\gamma = 105.631(5)°$
Volume	425.07(13) Å^3	
Z	2	
Density (calculated)	1.657 g/cm^3	
Absorption coefficient	0.158 mm^{-1}	
F(000)	212	
Crystal size	$0.20 \times 0.30 \times 0.50$ mm^3	
Theta range for data collection	3.01 to 25.05°	
Index ranges	$-7 \le h \le 7$, $-8 \le k \le 8$, $-12 \le l \le 12$	
Reflections collected	4137	
Independent reflections	1479 [R(int) = 0.0293]	
Completeness to theta = 25.05°	98.5%	
Absorption correction	Multiscan	
Max. and min. transmission	0.9691 and 0.8198	

https://doi.org/10.1017/S0885715618000829 Published online by Cambridge University Press

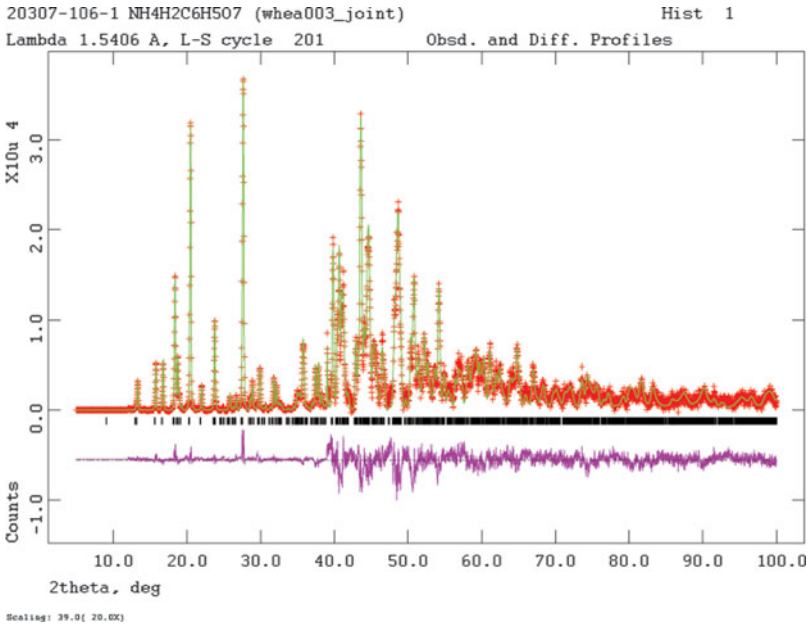

Figure 2. (Color online) The Rietveld plot for the refinement of $(NH_4)H_2C_6H_5O_7$. The red crosses represent the observed data points, and the green line is the calculated pattern. The magenta curve is the difference pattern, plotted at the same vertical scale as the other patterns. The vertical scale has been multiplied by a factor of 20 for $2\theta > 39.0°$. The row of black tick marks indicates the calculated reflection positions.

9 restraints) yielded the residuals $R_{wp} = 0.0719$, $R_p = 0.0551$, and $\chi^2 = 5.116$. The largest peak (0.67 Å from C3) and hole (0.00 Å from H22) in the difference Fourier map were 0.28 and -0.28 eÅ^{-3}, respectively. The Rietveld plot is included as Figure 2.

$(NH_4)_2HC_6H_5O_7$. Diammonium hydrogen citrate (Fisher lot #995047) was obtained from the chemistry stockroom at North Central College. A portion of the sample was ground in a mortar and pestle and sieved to <400 mesh. The powder pattern was measured on a PANalytical Empyrean diffractometer equipped with an incident-beam focusing mirror and an X'Celerator detector. The pattern (1–50°2θ, 0.0167113° steps, 4 s/step, 1/4° divergence slit, 0.02 radian Soller slits) was measured from a rotated 0.7 mm capillary using Mo Kα radiation. The powder pattern corresponded to that calculated from the crystal structure (Figure 2). A Rietveld refinement using the fixed ZZZSAC01 structure was carried out to determine the lattice parameters and profile coefficients.

$(NH_4)_3C_6H_5O_7$. Triammonium citrate (Sigma-Aldrich lot #BCBS1296) was obtained from the chemistry stockroom at North Central College. A portion of the sample was ground in a mortar and pestle and sieved to <400 mesh. The powder pattern was measured on a PANalytical Empyrean diffractometer equipped with an incident-beam focusing mirror and an X'Celerator detector. The pattern (1–50° 2θ, 0.0167113° steps, 4 s/step, 1/4° divergence slit, 0.02 radian Soller slits) was measured from a rotated 0.7 mm capillary using MoK_α radiation.

The pattern was indexed on a primitive monoclinic unit cell with $a = 6.077$, $b = 13.375$, $c = 13.534$ Å, $\beta = 92.53°$, $V = 1103.4$ Å^3, and $Z = 4$ using DICVOL as incorporated into FOX. The suggested space group was $P2_1/c$, which was confirmed by sa uccessful solution and refinement of the structure. The structure was solved with FOX ($\sin\theta/\lambda_{max} = 0.40$ Å^{-1}), using a citrate anion and 3 N atoms as fragments. The success rate was ~30% of the multiple runs.

Subsequent to the solution using powder data, poor-quality single crystals were isolated from the reagent bottle. A crystal approximately $0.40 \times 0.40 \times 0.40$ mm^3 was mounted in a Bruker SMART X2S diffractometer, and a single crystal data set was collected at 300 K using MoK_α radiation. Data collection information is summarized in Table II. A data set was collected from another crystal at 200 K to determine the lattice parameters.

Since the single crystal and powder data sets were collected at the same temperature, a joint refinement using both data sets was carried out using GSAS (Larson and Von Dreele, 2004; Toby, 2001). Only the 5.0–42.0° portion of the powder pattern was included in the refinement (d_{min} = 0.989 Å). The C, N, and O atoms were refined independently and anisotropically. All non-H bond distances and angles were subjected to restraints. The C-C bonds between the terminal carboxyl carbon atoms and the adjacent carbon atoms were restrained at 1.51(2) Å, the C-C bonds between the central carbon atom and the adjacent carbon atoms at 1.54(1) Å, the C-C bond between the central carbon atom and the central carboxyl carbon at 1.55(1) Å, the C-O bond to the hydroxyl group at 1.43(3) Å, and the C-O bonds in the carboxylate groups at 1.25(2) Å. The tetrahedral carbon bond angles were restrained at 109(3)°, and the angles in the planar carboxyl groups at 120 (3)°. The C-H bond distances were restrained to 1.00(3) Å, and the N-H distances to 0.90(3) Å. The hydrogen atoms were refined isotropically, with common U_{iso} based on chemical similarity. The peak profiles were described using profile function #4 (Thompson *et al.*, 1987; Finger *et al.*, 1994),

TABLE II. Room-temperature data collection for $(NH_4)_3C_6H_5O_7$.

Identification code	n3cit	
Empirical formula	$C_6H_{17}N_3O_7$	
Temperature	300(2) K	
Wavelength	0.70973 Å	
Crystal system	Monoclinic	
Space group	$P2_1/c$	
Unit cell dimensions	$a = 6.0626(7)$ Å	$\alpha = 90°$
	$b = 13.3191(17)$ Å	$\beta = 92.609(4)°$
	$c = 13.4933(17)$ Å	$\gamma = 90°$
Volume	1088.4(4) Å^3	
Crystal size	$0.40 \times 0.40 \times 0.40$ mm^3	
Reflections collected	7043	

https://doi.org/10.1017/S0885715618000829 Published online by Cambridge University Press

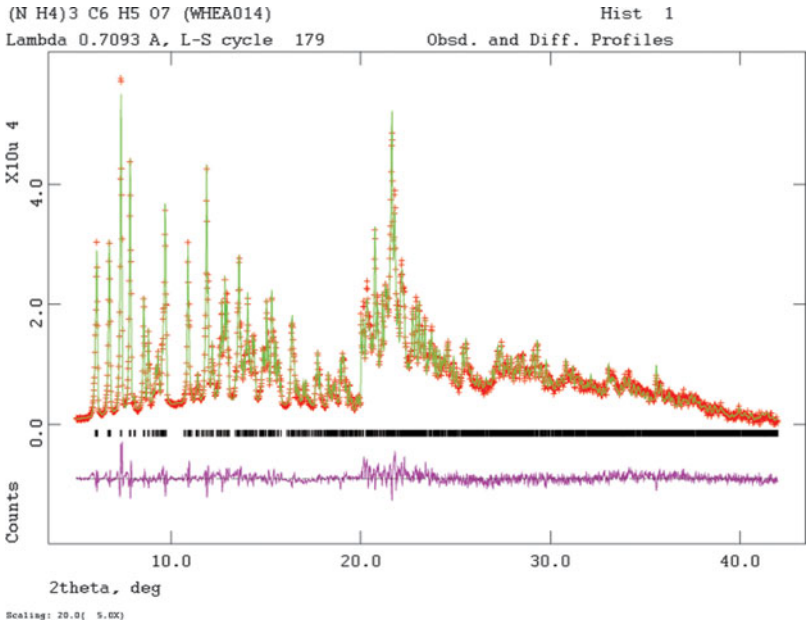

Figure 3. (Color online) The Rietveld plot for the refinement of $(NH_4)_3C_6H_5O_7$. The red crosses represent the observed data points, and the green line is the calculated pattern. The magenta curve is the difference pattern, plotted at the same vertical scale as the other patterns. The vertical scale has been multiplied by a factor of 5 for $2\theta > 20.0°$. The row of black tick marks indicates the calculated reflection positions.

which includes the Stephens (1999) anisotropic strain broadening model. The background was modeled using a 1-term shifted Chebyshev polynomial and a 6-term diffuse scattering function to model the capillary and any amorphous component. A 2nd-order spherical harmonic model was included; the refined texture index was 1.005, so preferred orientation was not significant in the powder specimen. The final refinement of 215 variables using 11614 observations (2214 powder data points, 9354 single crystal reflections, and 46 restraints) yielded the residuals $R_{wp} = 0.0447$, $R_p = 0.0341$, and $\chi^2 = 9.703$. The single crystal $R_w(F_o)$ was 0.073. The largest peak (1.40 Å from N21) and hole (1.44 Å from O15) in the difference Fourier map were 0.28 and $-0.26\ e\text{Å}^{-3}$, respectively. The Rietveld plot is included as Figure 3. The overall fit is excellent; the good signal/noise and the restraints result in a relatively high reduced χ^2 to accompany the low R_{wp}. The largest errors in the fit are in the shapes of some of the peaks.

Density functional geometry optimizations (fixed experimental unit cells) of all three structures were carried out

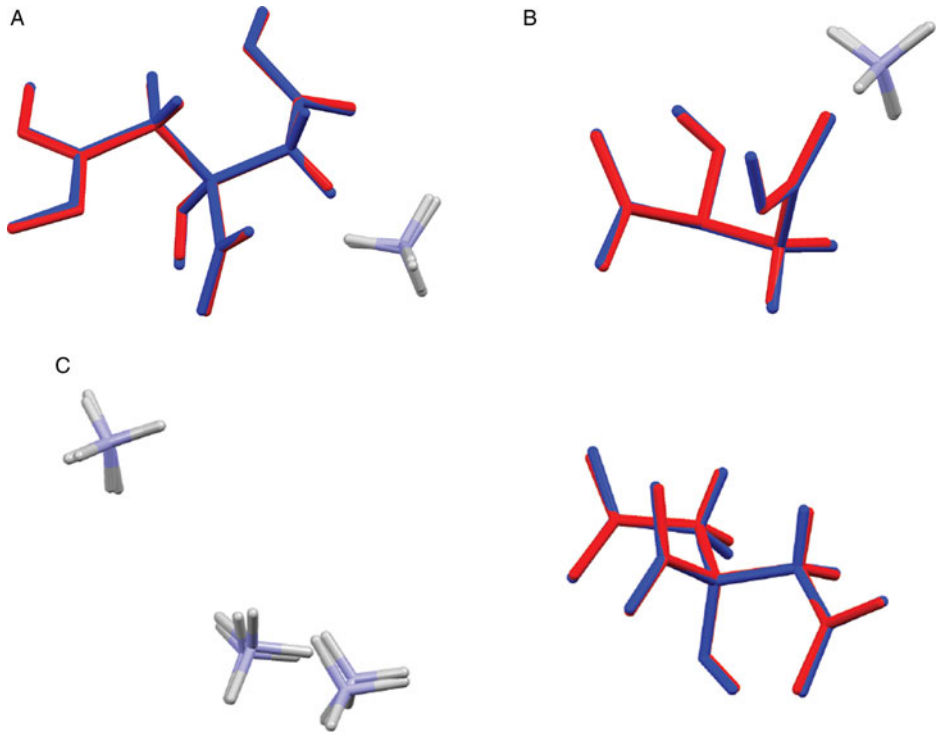

Figure 4. (Color online) (a) Comparison of the refined and optimized structures of $(NH_4)H_2C_6H_5O_7$. The Rietveld/single crystal refined structure is in red, and the density functional theory (DFT)-optimized structure is in blue. (b) Comparison of the refined and optimized structures of $(NH_4)_2HC_6H_5O_7$. The Rietveld/single crystal refined structure is in red, and the DFT-optimized structure is in blue. (c). Comparison of the refined and optimized structures of $(NH_4)_3C_6H_5O_7$. The Rietveld/single crystal refined structure is in red, and the DFT-optimized structure is in blue.

https://doi.org/10.1017/S0885715618000829 Published online by Cambridge University Press

using CRYSTAL14 (Dovesi *et al*., 2014). The basis sets for the H, C, N, and O atoms were those of Peintinger *et al*. (2013). The calculations were run on eight 2.1 GHz Xeon cores (each with 6 Gb RAM) of a 304-core Dell Linux cluster at IIT, used 8 *k*-points and the B3LYP functional, and took ~2–3 days (66 h/$(NH_4)H_2C_6H_5O_7$, 43 h/$(NH_4)_2HC_6H_5O_7$, 57 h/$(NH_4)_3C_6H_5O_7$).

For $(NH_4)H_2C_6H_5O_7$ and $(NH_4)_3C_6H_5O_7$, density functional optimizations (fixed experimental unit cells) were also carried out using VASP (Kresse and Furthmüller, 1996) through the MedeA graphical interface (Materials Design, 2016). The calculations were carried out on 8 2.4 GHz processors (each with 4 Gb RAM) of a 64-processor HP Proliant DL580 Generation 7 Linux cluster at North Central College. The calculation used the GGA-PBE functional, a planewave

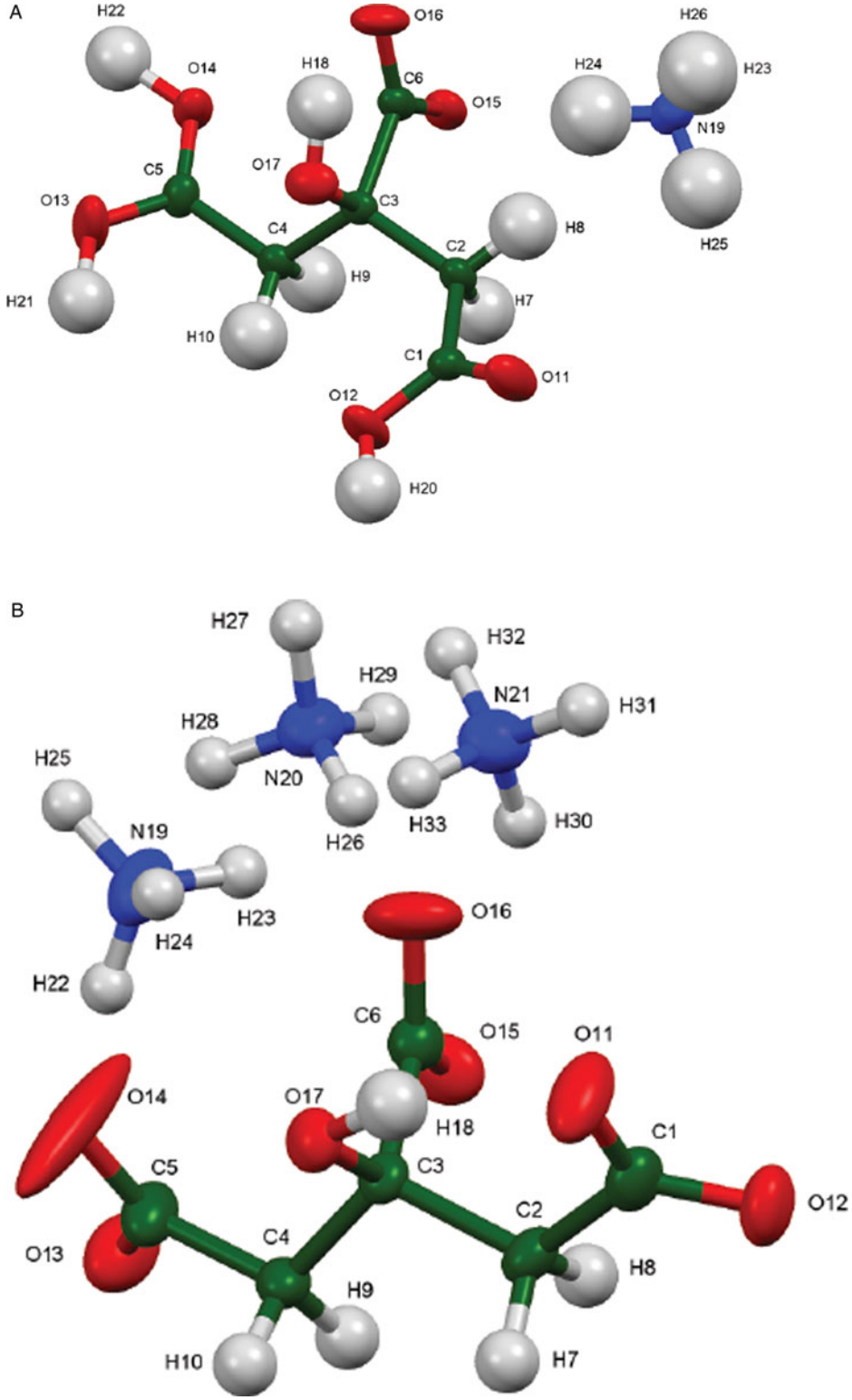

Figure 5. (Color online) (a) The asymmetric unit of $(NH_4)H_2C_6H_5O_7$, with the atom numbering. The atoms are represented by 50% probability ellipsoids (b) The asymmetric unit of $(NH_4)_3C_6H_5O_7$, with the atom numbering. The atoms are represented by 50% probability ellipsoids.

https://doi.org/10.1017/S0885715618000829 Published online by Cambridge University Press

cutoff energy of 400 eV, and a *k*-point spacing of 0.5 $Å^{-1}$ ($3 \times 2 \times 2$ and $3 \times 1 \times 1$ *k*-points), and took 0.7 and 1.6 h.

III. RESULTS AND DISCUSSION

The refined atom coordinates for all three compounds and the coordinates from the density functional theory (DFT) optimizations are reported in the CIFs attached as Supplementary Material. For $(NH_4)H_2C_6H_5O_7$ and $(NH_4)_3C_6H_5O_7$ (the new structures solved using powder data), the optimizations were carried out using both CRYSTAL14 and VASP. The fractional coordinates of the nitrogen atoms of the ammonium ions were identical (to within 0.001 Å) and the root-mean-square Cartesian displacements of the non-H atoms in the citrate anions were 0.027 and 0.012 Å, respectively. The two programs yield essentially identical structures. Since it is easier to analyze the hydrogen bonds using the CRYSTAL14 output, this discussion will concentrate on those optimized structures.

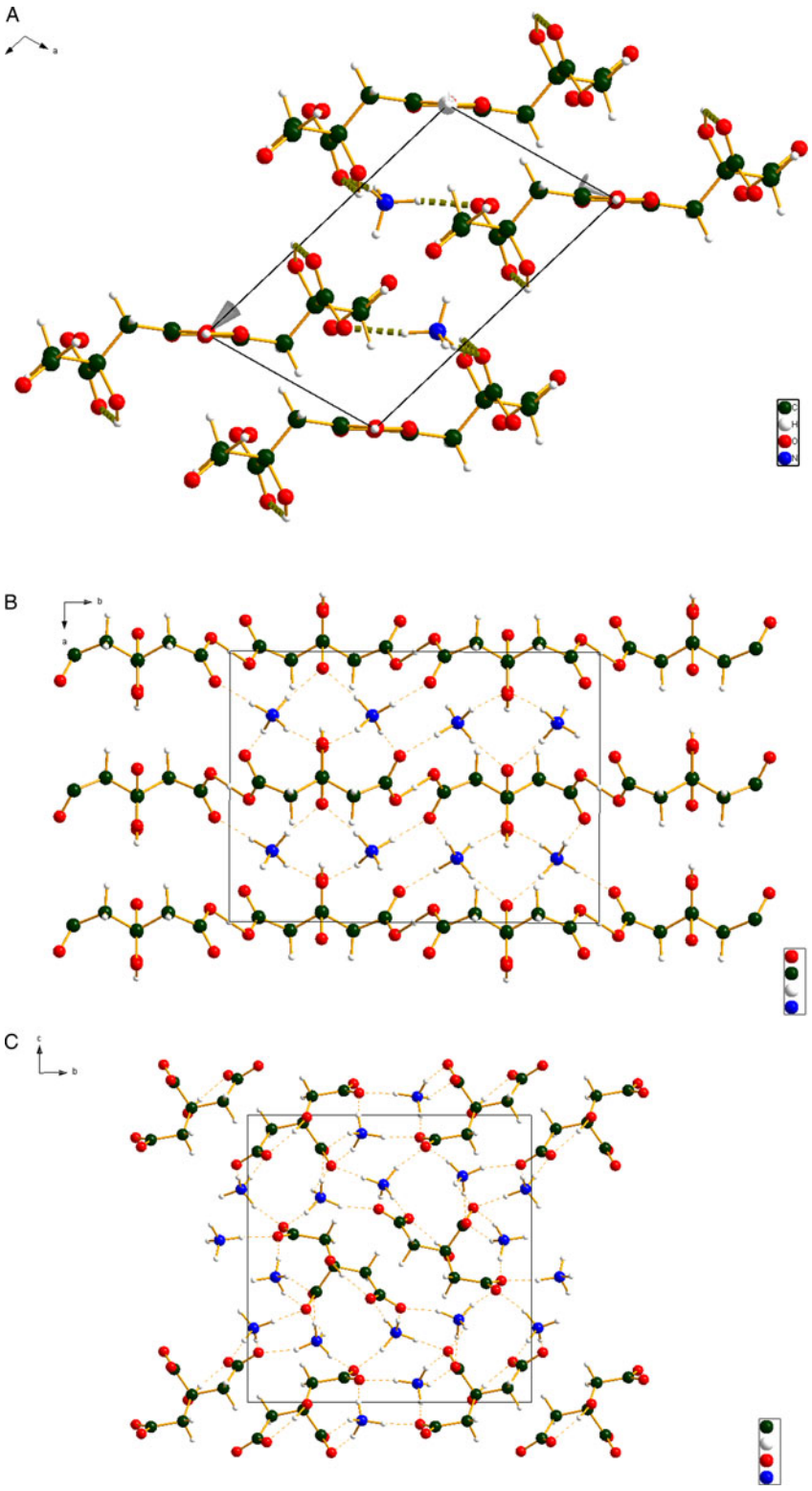

Figure 6. Color online (a) The crystal structure of $(NH_4)H_2C_6H_5O_7$, viewed down the *b*-axis. (b) The crystal structure of $(NH_4)_2HC_6H_5O_7$, viewed down the *c*-axis. (c) The crystal structure of $(NH_4)_3C_6H_5O_7$, viewed down the *a*-axis.

https://doi.org/10.1017/S0885715618000829 Published online by Cambridge University Press

TABLE III. Hydrogen bonds (CRYSTAL14) in ammonium dihydrogen citrate.

H-Bond	D-H, Å	H···A, Å	D····A, Å	D-H···A,◦	Overlap, *e*	E, kcal/mol
N19-H26···O17	1.031	1.919	2.939	169.8	0.045	4.9
N19-H25···O16	1.038	1.773	2.787	164.2	0.047	5.0
N19-H24···O15	1.031	1.874	2.899	172.5	0.039	4.6
N19-H23···O11	1.022	2.296	3.005	91.1	0.013	2.6
O14-H22-O14	1.207	1.207	2.414	180.0	0.151	21.2
O13-H21-O13	1.204	1.204	2.408	180.0	0.173	22.7
O12-H20···O15	1.025	1.538	2.558	173.2	0.059	13.3
O17-H18···O16	0.978*	1.929	2.579	121.5	0.043	11.3
C2-H8···O11	1.088	2.261	3.340	171.2	0.012	

* = intramolecular.

Comparing the experimental and DFT-optimized structures, the root-mean-square Cartesian displacements of the non-hydrogen atoms in the citrates of $(NH_4)H_2C_6H_5O_7$, $(NH_4)_2HC_6H_5O_7$, and $(NH_4)_3C_6H_5O_7$ are 0.0722, 0.0206, and 0.1021 Å respectively (Figures 4a, b, c). The excellent agreement between the refined and optimized structures is evidence that the experimental structures are correct (van de Streek and Neumann, 2014). The agreement for the single-crystal structure is notably better than for the two powder structures. The following discussion uses the DFT-optimized structures.

Almost all of the bond distances, bond angles, and torsion angles in the citrate anions fall within the normal ranges indicated by a Mercury Mogul Geometry check (Macrae *et al*., 2008). Only the O11-C1-C2-C3 and C4-C3-C2-C1 torsion angles in $(NH_4)H_2C_6H_5O_7$ are flagged as unusual. As noted in Rammohan and Kaduk (2018), the carboxyl torsion angles in citrates cover all possible values, so the occurrence of this angle in a minor part of the distribution is not a cause for concern. The citrate in $(NH_4)H_2C_6H_5O_7$ occurs in the *gauche/trans* conformation [Figure 5(a)], one of the two lowest-energy conformations of an isolated citrate (though a minority). The citrates in $(NH_4)_2HC_6H_5O_7$ and $(NH_4)_3C_6H_5O_7$ occur in the *trans/trans* conformation (Figure 5b).

The three crystal structures are illustrated in Figures 6(a)–6(c). As discussed below, all three structures are dominated by hydrogen bonding. The hydrophobic methylene groups lie adjacent to each other in the structures. In $(NH_4)_2HC_6H_5O_7$ the citrate anion lies on a mirror plane.

Analysis of the contributions to the total crystal energy in $(NH_4)_3C_6H_5O_7$ using the Forcite module of Materials Studio (Dassault, 2018) suggests that the intermolecular energy is dominated by electrostatic attractions, which in this force-field-based analysis include hydrogen bonds. The hydrogen bonds are better analyzed using the results of the DFT calculations. (Forcite was not able to accommodate the chains of strong H-bonds in $(NH_4)H_2C_6H_5O_7$ and $(NH_4)_2HC_6H_5O_7$.)

As expected, these crystal structures are dominated by N-H···O hydrogen bonds (Tables III, IV, and V), though O-H···O hydrogen bonds are also important. In $(NH_4)H_2C_6H_5O_7$ very strong (as measured by the Mulliken overlap populations) centrosymmetric charge-assisted O13-H21-O13 and O14-H22-O14 hydrogen bonds link one end of the citrate into chains along the *b*-axis. A more-normal (by the overlap population) O12-H20···O15 links the other end of the citrate to the central ionized carboxyl group. Ionization of the central carboxyl group first is the normal pattern of ionization in the solid state (Rammohan and Kaduk, 2018). The hydroxyl group forms an intramolecular hydrogen bond to the central carboxylate. The N19-H23···O11 hydrogen bond is weaker than the other four, reflected in its length, angle, and overlap population. In $(NH_4)_2HC_6H_5O_7$, the very strong centrosymmetric O1-H8-O1 hydrogen bonds link the citrates into zigzag chains along the *b*-axis. The citrates occupy layers parallel to the *bc* plane, and the ammonium ions link the layers through N-H···O hydrogen bonds. All four of the N-H···O hydrogen bonds have similar strength. The hydroxyl groups also form an intramolecular hydrogen bond to the central ionized carboxylate and $(NH_4)_2HC_6H_5O_7$, hydroxyl groups. In $(NH_4)_3C_6H_5O_7$, the hydroxyl group forms a hydrogen bond to a terminal carboxylate, perhaps because each of the oxygen atoms of the central carboxylate acts as an acceptor in two N-H···O hydrogen bonds. The hydrogen bond involving H30 is weaker than the other 11 N-H···O hydrogen bonds, reflected by its smaller angle.

The unit cell energies of the three compounds calculated by CRYSTAL14 provide an opportunity to derive a correlation between the Mulliken overlap population in an N-H···O hydrogen bond and the energy of that bond. Under the assumption that the energy/citrate is a linear combination of

TABLE IV. Hydrogen bonds (CRYSTAL14) in diammonium hydrogen citrate.

H-Bond	D-H, Å	H···A, Å	D····A, Å	D-H···A,◦	Overlap, *e*	E, kcal/mol
O1-H1-O1	1.198	1.198	2.396	180.0	0.171	22.6
N1-H7···O2	1.039	1.764	2.801	174.6	0.052	5.3
N1-H6···O3	1.029	1.929	2.937	165.6	0.035	4.3
N1-H5···O4	1.031	1.854	2.862	164.9	0.038	4.5
N1-H4···O2	1.034	1.839	2.869	174.1	0.045	4.9
O5-H1···O3	0.975*	1.876	2.552	124.0	0.032	9.8

* = intramolecular.

https://doi.org/10.1017/S0885715618000829 Published online by Cambridge University Press

TABLE V. Hydrogen bonds (CRYSTAL14) in triammonium citrate.

H-Bond	D-H, Å	H···A, Å	D····A, Å	D-H···A,◦	Overlap, *e*	E, kcal/mol
O17-H18···O11	0.983*	1.756	2.685	146.9	0.050	12.2
N19-H22···O14	1.030	1.887	2.845	153.3	0.034	4.2
N19-H23···O16	1.029	1.855	2.841	159.2	0.030	4.0
N19-H24···O15	1.025	1.914	2.846	149.7	0.032	4.1
N19-H25···O14	1.044	1.725	2.754	167.8	0.057	5.5
N20-H26···O16	1.036	1.800	2.832	174.0	0.038	4.5
N20-H27···O11	1.045	1.717	2.761	176.4	0.066	5.9
N20-H28···O13	1.041	1.738	2.759	165.4	0.060	5.6
N20-H29···O12	1.041	1.731	2.756	167.4	0.061	5.7
N21-H30···O16	1.022	2.031	2.842	134.5	0.019	3.2
N21-H31···O13	1.036	1.795	2.780	157.4	0.042	4.7
N21-H32···O12	1.033	1.813	2.792	156.8	0.042	4.7
N21-H33···O15	1.042	1.724	2.764	175.9	0.062	5.7

TABLE VI. Lattice parameters of $(NH_4)_3C_6H_5O_7$.

	200 K	300 K	Expansion
a, Å	6.0513(16)	6.0867(2)	0.58%
b, Å	13.2905(41)	13.3914(4)	0.76%
c, Å	13.4447(42)	14.5497(5)	0.78%
β,◦	92.660(10)	92.521(2)	
V, Å^3	1080.13(89)	1103.36(9)	2.15%

the energies of the citrate anion, the ammonium cations, the N-H···O hydrogen bonds, and the O-H···O hydrogen bonds (the energies of which were calculated using the correlation in Rammohan and Kaduk, 2018), some simple algebra results in an average N-H···O hydrogen bond energy of −4.79 kcal/mole. The average Mulliken overlap population of the N-H···O hydrogen bonds in these compounds is 0.043(13) *e*. Assuming the previous correlation that the energy of a hydrogen bond is proportional to the square root of the overlap population in the H···A bond (Rammohan and Kaduk, 2018; Kaduk, 2002), we derive:

$$E(\mathrm{N-H\cdots O})(\mathrm{kcal/mole}) = 23.1(\mathrm{overlap})^{1/2}$$

This correlation was used to calculate the hydrogen bond energies in TABLES III–V.

The lattice parameters of $(NH_4)_3C_6H_5O_7$ were determined at 200 K from a single crystal and at 300 K using powder data (Table VI). The expansion between the two temperatures is nearly isotropic.

The Bravais-Friedel-Donnay-Harker (Bravais, 1866; Friedel, 1907; Donnay and Harker, 1937; calculated in *Mercury*) morphology suggests that we might expect platy morphology for $(NH_4)H_2C_6H_5O_7$ with {001} as the major faces, blocky morphology for $(NH_4)_2HC_6H_5O_7$ with {020} as major faces, and {011} plates and/or {100} needles for $(NH_4)_3C_6H_5O_7$. As noted in the experimental section, preferred orientation was not severe for any of these samples.

As shown in Figure 1, the powder pattern reported in PDF entry 00-045-1540 for "triammonium citrate" corresponds to the experimental and calculated patterns for diammonium hydrogen citrate. The compound was mis-characterized by Venkateshwarlu *et al*. (1993). An authentic powder pattern for triammonium citrate (as well as one for ammonium dihydrogen citrate) have been submitted to the International Centre for Diffraction Data for inclusion in the PDF.

SUPPLEMENTARY MATERIAL

The supplementary material for this article can be found at https://doi.org/10.1017/S0885715618000829.

ACKNOWLEDGEMENTS

The authors thank Andrey Rogachev for the use of computing resources at IIT.

Altomare, A., Cuocci, C., Giacovazzo, C., Moliterni, A., Rizzi, R., Corriero, N., and Falcicchio, A. (**2013**). "EXPO2013: a kit of tools for phasing crystal structures from powder data," J. Appl. Crystallogr. **46**, 1231–1235.

Andrade, L. C. R., Costa, M. M. R., Paixão, J. A., Santos, M. L., Agostinho Moreira, J., and Almeida, A. (**2002**). "Crystal structure of diammonium hydrogen-2-hydroxy-1,2,3-propanetricarboxylate, $(NH_4)_2(C_6H_6O_7)$," Z. Kristallogr. NCS **217**, 537–538.

Bravais, A. (**1866**). *Etudes Cristallographiques* (Gauthier Villars, Paris).

Cigler, A. J. and Kaduk, J. A. (**2018**). "Dilithium (citrate) crystals and their relatives," Acta Cryst. Sect. C **74**(10), 1160–1170.

Dassault Systèmes (**2018**). *Materials Studio 2018* (BIOVIA, San Diego CA).

Donnay, J. D. H. and Harker, D. (**1937**). "A new law of crystal morphology extending the law of Bravais," Amer. Mineral. **22**, 446–467.

Dovesi, R., Orlando, R., Erba, A., Zicovich-Wilson, C. M., Civalleri, B., Casassa, S., Maschio, L., Ferrabone, M., De La Pierre, M., D-Arco, P., Noël, Y., Causà, M., and Kirtman, B. (**2014**). "CRYSTAL14: a program for the ab initio investigation of crystalline solids," Int. J. Quantum Chem. **114**, 1287–1317.

Favre-Nicolin, V. and Černý, R. (**2002**). FOX, "Free Objects for crystallography: a modular approach to ab initio structure determination from powder diffraction," J. Appl. Crystallogr. **35**, 734–743.

Fawcett, T. G., Kabekkodu, S. N., Blanton, J. R., and Blanton, T. N. (**2017**). "Chemical analysis by diffraction: the Powder Diffraction File™," Powder Diffr. **32**(2), 63–71.

Finger, L. W., Cox, D. E., and Jephcoat, A. P. (**1994**). "A correction for powder diffraction peak asymmetry due to axial divergence," J. Appl. Crystallogr. **27**(6), 892–900.

Friedel, G. (**1907**). "Etudes sur la loi de Bravais," Bull. Soc. Fr. Mineral. **30**, 326–455.

Gong, P. (**1980**). "Ammonium citrate," ICDD Grant-in-Aid, PDF entry 00-031-1531.

Groom, C. R., Bruno, I. J., Lightfoot, M. P., and Ward, S. C. (**2016**). "The Cambridge Structural Database," Acta Crystallogr. Sect. B: Struct. Sci., Cryst. Eng. Mater. **72**, 171–179.

Kaduk, J. A. (**2002**). "Use of the inorganic crystal structure database as a problem solving tool," Acta Cryst. Sect B: Struct. Sci. **58**, 370–379.

Kaduk, J. A. and Stern, C. (**2016a**). "Potassium dihydrogen citrate," CSD Refcodes ZZZEJE01 and ZZZEJE02.

https://doi.org/10.1017/S0885715618000829 Published online by Cambridge University Press

Kaduk, J. A. and Stern, C. (**2016b**). "Potassium dihydrogen citrate dihydrate," CSD Refcodes FAFMAD and FAFMAD01.
Kresse, G., and Furthmüller, J. (**1996**). "Efficiency of Ab-initio total energy calculations for metals and semiconductors using a plane-wave basis Set," Comput. Mater. Sci. **6**, 15–50.
Larson, A. C. and Von Dreele, R. B. (**2004**). *General Structure Analysis System (GSAS)* (Los Alamos National Laboratory Report LAUR 86-784).
Love, W. E. and Patterson, A. L. (**1960**). "X-ray crystal analysis of the substrates of aconitase. III. Crystallization, cell constants, and space groups of some alkali citrates," Acta Crystallogr. **13**(5), 426–428.
Macrae, C. F., Bruno, I. J., Chisholm, J. A., Edington, P. R., McCabe, P., Pidcock, E., Rodriguez-Monge, L., Taylor, R., van de Streek, J., and Wood, P. A. (**2008**). "Mercury CSD 2.0 – new features for the visualization and investigation of crystal structures," J. Appl. Crystallogr. **41**, 466–470.
Materials Design (**2016**). *MedeA 2.20.4* (Materials Design Inc., Angel Fire NM).
Peintinger, M. F., Vilela Oliveira, D., and Bredow, T. (**2013**). "Consistent Gaussian basis sets of triple-zeta valence with polarization quality for solid-state calculations," J. Comput. Chem. **34**, 451–459.
Rammohan, A. and Kaduk, J. A. (**2016a**). "Sodium potassium hydrogen citrate, $NaKHC_6H_5O_7$," Acta Cryst. E **72**, 170–173.
Rammohan, A. and Kaduk, J. A. (**2016b**). "Sodium dipotassium citrate, $NaK_2C_6H_5O_7$," Acta Cryst. E **72**, 403–406.
Rammohan, A. and Kaduk, J. A. (**2016c**). "Trisodium citrate, $Na_3(C_6H_5O_7)$," Acta Cryst. E **72**, 793–796.
Rammohan, A. and Kaduk, J. A. (**2016d**). "A second polymorph of sodium dihydrogen citrate, $NaH_2C_6H_5O_7$: structure solution from powder diffraction data and DFT comparison," Acta Cryst. E **72**, 854–857.
Rammohan, A. and Kaduk, J. A. (**2016e**). "Crystal structure of anhydrous tripotassium citrate from laboratory X-ray powder diffraction data and DFT comparison," Acta Cryst. E **72**, 1159–1162.
Rammohan, A., Sarjeant, A. A., and Kaduk, J. A. (**2016**). "Disodium hydrogen citrate sesquihydrate, $Na_2HC_6H_5O_7(H_2O)_{1.5}$," Acta Cryst. E **72**, 943–946.
Rammohan, A. and Kaduk, J. A. (**2017a**). "Crystal structure of dirubidium hydrogen citrate from laboratory X-ray powder diffraction data and DFT comparison," Acta Cryst. E **73**, 92–95.
Rammohan, A. and Kaduk, J. A. (**2017b**). "Crystal structure of trirubidium citrate monohydrate from laboratory X-ray powder diffraction data and DFT comparison," Acta Cryst. E **73**, 227–230.
Rammohan, A. and Kaduk, J. A. (**2017c**). "Crystal structure of trirubidium citrate from laboratory X-ray powder diffraction data and DFT comparison," Acta Cryst. E **73**, 250–253.
Rammohan, A. and Kaduk, J. A. (**2017d**). "Crystal structure of pentasodium hydrogen dicitrate from synchrotron X-ray powder diffraction data and DFT comparison," Acta Cryst. E **73**, 286–290.
Rammohan, A. and Kaduk, J. A. (**2017e**). "Crystal structure of caesium dihydrogen citrate from laboratory X-ray powder diffraction data and DFT comparison," Acta Cryst. E **73**, 133–136.
Rammohan, A. and Kaduk, J. A. (**2017f**). CSD Communication 1525884.
Rammohan, A. and Kaduk, J. A. (**2018**). "Crystal structures of alkali metal (Group 1) citrate salts," accepted by *Acta Cryst. Sect. B: Cryst. Eng. Mater./Acta Cryst. Sect. C: Struct. Chem.*; hw5048.
Rammohan, A., Sarjeant, A. A., and Kaduk, J. A. (**2017a**). "Crystal structure of dicaesium hydrogen citrate from laboratory single-crystal and powder X-ray diffraction data and DFT comparison," Acta Cryst. E **73**, 231–234.
Rammohan, A., Sarjeant, A. A., and Kaduk, J. A. (**2017b**). "Tricaesium citrate monohydrate, $Cs_3C_6H_5O_7 \cdot H_2O$: crystal structure and DFT comparison," Acta Cryst. E **73**, 520–523.
Stephens, P. W. (**1999**). "Phenomenological model of anisotropic peak broadening in powder diffraction," J. Appl. Crystallogr. **32**, 281–289.
Thompson, P., Cox, D. E., and Hastings, J. B. (**1987**). "Rietveld refinement of Debye-Scherrer synchrotron X-ray data from Al_2O_3," J. Appl. Crystallogr. **20**(2), 79–83.
Toby, B. H. (**2001**). "EXPGUI, a graphical user interface for GSAS," J. Appl. Crystallogr. **34**, 210–213.
van de Streek, J. and Neumann, M. A. (**2014**). "Validation of molecular crystal structures from powder diffraction data with dispersion-corrected density functional theory (DFT-D)," Acta Cryst. Sect. B: Struct. Sci., Cryst. Eng. Mater., **70**(6), 1020–1032.
Venkateshwarlu, M., Bhaskar Rao, T., and Kishan Rao, K. (**1989**). "Growth and characterization of triammonium citrate," Bull. Mater. Sci. **12**(2), 146–146.
Venkateshwarlu, M., Hussain, K. A., and Bhaskar Rao, T. (**1993**). "X-ray data for triammonium citrate," Powder Diffr. **8**(3), 173–174.
Visser, J. (**1979**). "Ammonium hydrogen citrate," ICDD Grant-in-Aid, PDF entry 00-031-1529.

https://doi.org/10.1017/S0885715618000829 Published online by Cambridge University Press